ATMOSPHERIC CHEMISTRY

Atmospheric new particle formation from sulfuric acid and amines in a Chinese megacity

Lei Yao[1]*, Olga Garmash[2]*, Federico Bianchi[2,3], Jun Zheng[4], Chao Yan[2], Jenni Kontkanen[2,5], Heikki Junninen[2,6], Stephany Buenrostro Mazon[2], Mikael Ehn[2], Pauli Paasonen[2], Mikko Sipilä[2], Mingyi Wang[1]†, Xinke Wang[1], Shan Xiao[1]‡, Hangfei Chen[1], Yiqun Lu[1], Bowen Zhang[1], Dongfang Wang[7], Qingyan Fu[7], Fuhai Geng[8], Li Li[9], Hongli Wang[9], Liping Qiao[9], Xin Yang[1,10,11], Jianmin Chen[1,10,11], Veli-Matti Kerminen[2], Tuukka Petäjä[2,12], Douglas R. Worsnop[2,13], Markku Kulmala[2,3], Lin Wang[1,10,11,14]§

Atmospheric new particle formation (NPF) is an important global phenomenon that is nevertheless sensitive to ambient conditions. According to both observation and theoretical arguments, NPF usually requires a relatively high sulfuric acid (H_2SO_4) concentration to promote the formation of new particles and a low preexisting aerosol loading to minimize the sink of new particles. We investigated NPF in Shanghai and were able to observe both precursor vapors (H_2SO_4) and initial clusters at a molecular level in a megacity. High NPF rates were observed to coincide with several familiar markers suggestive of H_2SO_4–dimethylamine (DMA)–water (H_2O) nucleation, including sulfuric acid dimers and H_2SO_4-DMA clusters. In a cluster kinetics simulation, the observed concentration of sulfuric acid was high enough to explain the particle growth to ~3 nanometers under the very high condensation sink, whereas the subsequent higher growth rate beyond this size is believed to result from the added contribution of condensing organic species. These findings will help in understanding urban NPF and its air quality and climate effects, as well as in formulating policies to mitigate secondary particle formation in China.

Atmospheric nucleation and subsequent growth of newly formed particles are a major source of atmospheric aerosol particles in terms of their number concentration (*1*–*4*), which can affect the climate directly and indirectly (*5*). During the past several years, knowledge about new particle formation (NPF) has increased through laboratory experiments, especially those carried out in the Cosmics Leaving Outdoor Droplets (CLOUD) chamber at CERN (*6*–*11*). Detailed mechanisms for atmospheric nucleation have been proposed for a few locations with low background aerosol loadings (*8*, *12*–*14*).

It is still a puzzle why and how NPF occurs in a highly polluted urban atmosphere like those in Chinese megacities (*15*, *16*). The very high aerosol concentration, causing a large condensation sink (CS), should efficiently scavenge newly formed molecular clusters before they reach sizes of a few nanometers, except when the cluster growth rate (GR) is exceptionally high (*15*, *17*, *18*). However, even in highly polluted areas, such as Nanjing in eastern China, secondary aerosol production makes a dominant contribution to the total aerosol number load, and more than half of accumulation-mode aerosol particles have been estimated to be of secondary origin (*19*). The observation of frequent NPF events in megacities such as Beijing (*20*, *21*), Shanghai (*22*), and Nanjing (*23*) urges a major advance in our understanding of the physical and chemical mechanisms for NPF in a heavily polluted atmosphere, which would ultimately help us to improve the performance of global and regional models.

We performed measurements in the Chinese megacity Shanghai (fig. S1) to investigate the mechanisms and effects of atmospheric NPF. The first dataset includes long-term continuous observations between March 2014 and February 2016 of particle number size distributions down to ~1.2 nm and atmospheric trace gas concentrations. The instruments used during this period were one particle size magnifier (PSM), one nano-scanning mobility particle sizer (nano-SMPS), and one long-SMPS. The second set of data was recorded during an intensive campaign from December 2015 to February 2016 with additional mass spectrometric measurements of gas-phase aerosol precursors and clusters. During this period, we additionally used one neutral cluster and air ion spectrometer (NAIS) and one nitrate-based chemical ionization–atmospheric pressure interface–time-of-flight mass spectrometer (CI-APi-TOF) (*24*). These two complementary datasets provide both precise fingerprint-type details and the nucleation climatology that together elucidate the chemical and physical mechanisms for the observed NPF events.

During the long-term measurements, we identified 114 strong NPF events with maximum-to-background concentration ratios of >20 for sub–3-nm particles, corresponding to an NPF frequency of 15.6%. As shown in table S1, the formation rates of particles in the size range of 1.7 to 2 nm ($J_{1.7}$) and CS values in urban Shanghai are one to two orders of magnitude higher than typical values in the clean atmosphere (*15*, *22*). NPF events in urban Shanghai are favored on days with stronger solar radiation, higher ozone concentration, higher sulfuric acid concentration, lower relative humidity (RH), and less NO_x (fig. S2). The correlation with radiation, sulfuric acid, and ozone production indicates that the identified NPF events in Shanghai were generally photochemically induced. Lower RH is related to sunny days with strong radiation, which favor the formation of OH radicals and hence sulfuric acid (*25*). NO_x can react with peroxy radicals to compete with the autoxidation pathway, thereby hindering the formation of critical intermediates for NPF (*26*).

When looking at NPF at a molecular level, we found that naturally charged 2- to 4-nm ions (figs. S3b and S4) were scavenged by preexisting particles in Shanghai. This finding provided little information except that ion-induced nucleation was not responsible for the observed NPF events. The ion-induced contribution to NPF based on the calculated ratio of $J_{1.7}$(ion)/$J_{1.7}$(total) was 0.03% for negative ions and 0.05% for positive ions, respectively. We therefore concentrated on neutral compounds and clusters measured by using a nitrate-based CI-APi-TOF during the intensive campaign. The most notable observation was the highest signal of a sulfuric acid dimer, $H_2SO_4{\cdot}HSO_4^-$, ever observed in an ambient atmosphere [see also Kürten *et al.* (*27*)]. $H_2SO_4{\cdot}HSO_4^-$ detected by the nitrate-based CI-APi-TOF has previously been explained by the stabilization of the neutral sulfuric acid dimer in the real

[1]Shanghai Key Laboratory of Atmospheric Particle Pollution and Prevention (LAP[3]), Department of Environmental Science and Engineering, Fudan University, Shanghai 200433, China. [2]Institute for Atmospheric and Earth System Research/Physics, Faculty of Science, University of Helsinki, 00014 Helsinki, Finland. [3]Aerosol and Haze Laboratory, Beijing University of Chemical Technology, Beijing 100029, China. [4]Jiangsu Key Laboratory of Atmospheric Environment Monitoring and Pollution Control, Nanjing University of Information Science and Technology, Nanjing 210044, China. [5]Department of Environmental Science and Analytical Chemistry (ACES) and Bolin Centre for Climate Research, Stockholm University, 10691 Stockholm, Sweden. [6]Laboratory of Environmental Physics, Institute of Physics, University of Tartu, Tartu 50411, Estonia. [7]Shanghai Environmental Monitoring Center, Shanghai 200030, China. [8]Shanghai Meteorology Bureau, Shanghai 200135, China. [9]Shanghai Academy of Environmental Sciences, Shanghai 200233, China. [10]Institute of Atmospheric Sciences, Fudan University, Shanghai 200433, China. [11]Collaborative Innovation Center of Climate Change, Nanjing 210023, China. [12]Joint International Research Laboratory of Atmospheric and Earth System Sciences (JirLATEST), Nanjing University, Nanjing 210023, China. [13]Aerodyne Research, Billerica, MA 01821, USA. [14]Shanghai Institute of Pollution Control and Ecological Security, Shanghai 200092, China.
*These authors contributed equally to this work. †Present address: Center for Atmospheric Particle Studies, Carnegie Mellon University, Pittsburgh, PA 15213, USA. ‡Present address: Shanghai Qingning Environmental Planning and Design, Shanghai 200052, China.
§Corresponding author. Email: lin_wang@fudan.edu.cn

atmosphere by dimethylamine (DMA) (*6*, *9*, *28*) or by a molecule that works in the same way as DMA. During the process of charging by the NO_3^- reagent ions, DMA evaporated and one molecule of H_2SO_4 was replaced with one bisulfate ion, HSO_4^-. The particle formation rate plotted against the measured $H_2SO_4 \cdot HSO_4^-$ concentration is shown in Fig. 1A. A good correlation (correlation coefficient $r = 0.75$, $P < 0.001$) is evident for the dimer concentration exceeding 1×10^4 cm^{-3}. This suggests that the formation of atmospheric clusters giving a strong sulfuric acid dimer signal in the CI-APi-TOF was crucial for the observed nucleation processes.

Figure 1B presents the median sulfuric acid dimer concentration as a function of the sulfuric acid monomer concentration for NPF and nonevent days during the intensive campaign. Our measured dimer-to-monomer ratio is much larger than the corresponding theoretical maximum ratio because of ion-induced clustering (IIC) of sulfuric acid within the CI-APi-TOF ion reaction zone (*29*), being about one order of magnitude larger than previously reported ambient values when the sulfuric acid monomer concentration reached 1×10^7 molecule cm^{-3} (*27*, *29*). At this level of sulfuric acid concentration, our dimer-to-monomer ratio is close to a previous experimental observation from H_2SO_4-DMA-H_2O nucleation in the CLOUD experiment (*9*). Cluster kinetics simulations (see supplementary materials) for a kinetically limited H_2SO_4-DMA system show a qualitative agreement with our measured values, including the effect of CS on the dimer-to-monomer ratio (Fig. 1B). During NPF days, this ratio is larger and the CS is smaller, which is opposite to nonevent days. Very high CS values (>0.02 s^{-1}) seem to prevent NPF in Shanghai. However, values of ~0.01 to 0.02 s^{-1} with the observed GRs are expected to cause very high scavenging of small clusters, indicating that our knowledge of NPF under polluted conditions is still incomplete (*15*).

As suggested by other neutral clusters (Fig. 1C), the identity of the stabilizer for the sulfuric acid dimer is most likely DMA. Using the nitrate-based CI-APi-TOF, we observed large sulfuric acid clusters (trimer and tetramer) and sulfuric acid–DMA clusters consisting of up to four molecules of sulfuric acid and two molecules of DMA in the ambient atmosphere. However, because one or more DMA molecules could have evaporated after the charging of the parent neutral sulfuric acid–DMA cluster by reagent ions (*6*, *9*, *30*), we expect a larger number of DMA molecules in sulfuric acid–DMA clusters than observed here. On the other hand, the high particle GRs in

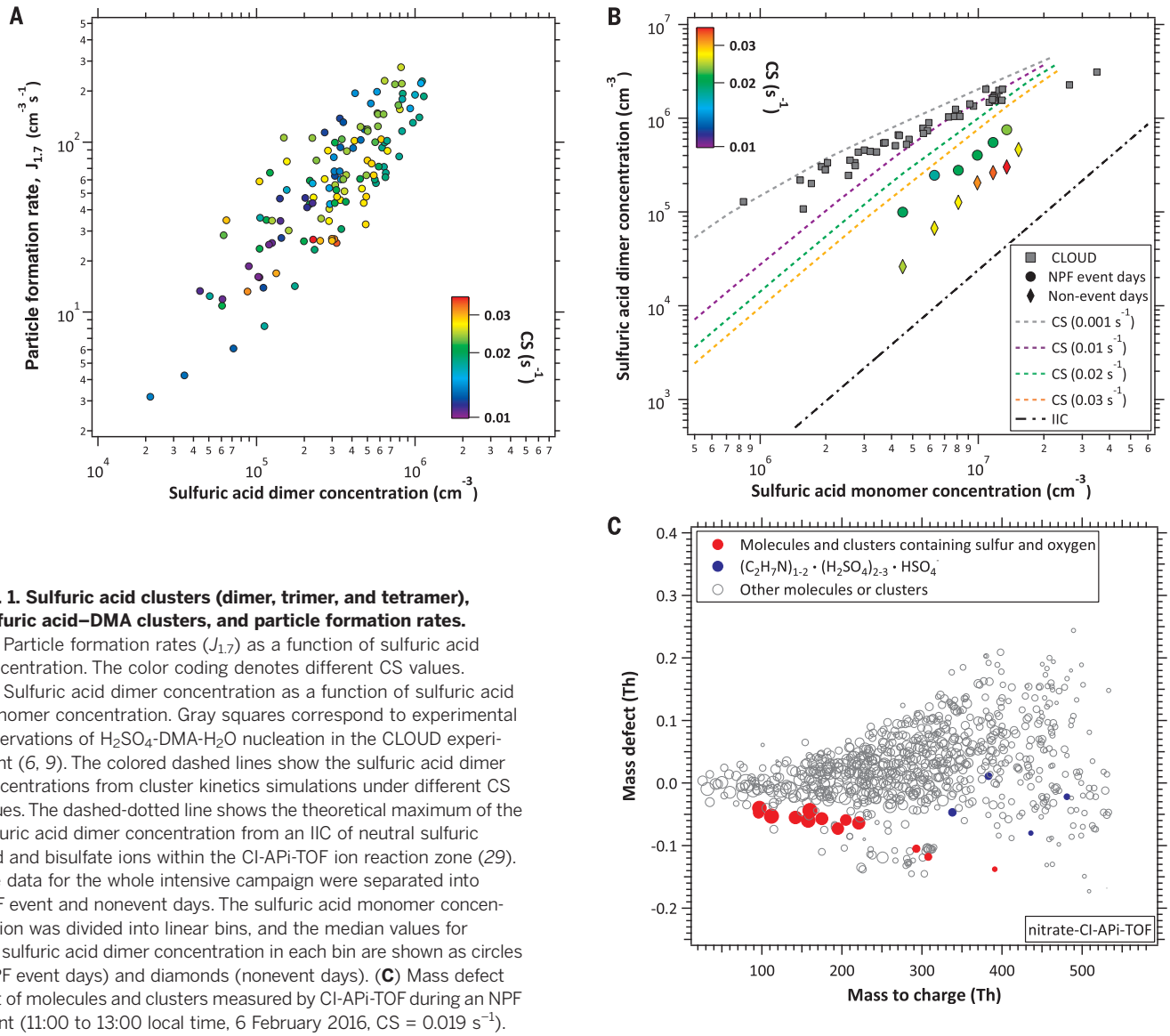

Fig. 1. Sulfuric acid clusters (dimer, trimer, and tetramer), sulfuric acid–DMA clusters, and particle formation rates. (**A**) Particle formation rates ($J_{1.7}$) as a function of sulfuric acid concentration. The color coding denotes different CS values. (**B**) Sulfuric acid dimer concentration as a function of sulfuric acid monomer concentration. Gray squares correspond to experimental observations of H_2SO_4-DMA-H_2O nucleation in the CLOUD experiment (*6*, *9*). The colored dashed lines show the sulfuric acid dimer concentrations from cluster kinetics simulations under different CS values. The dashed-dotted line shows the theoretical maximum of the sulfuric acid dimer concentration from an IIC of neutral sulfuric acid and bisulfate ions within the CI-APi-TOF ion reaction zone (*29*). The data for the whole intensive campaign were separated into NPF event and nonevent days. The sulfuric acid monomer concentration was divided into linear bins, and the median values for the sulfuric acid dimer concentration in each bin are shown as circles (NPF event days) and diamonds (nonevent days). (**C**) Mass defect plot of molecules and clusters measured by CI-APi-TOF during an NPF event (11:00 to 13:00 local time, 6 February 2016, CS = 0.019 s^{-1}). Data for compounds containing sulfur and oxygen (table S2), sulfuric acid–DMA clusters, and other molecules or clusters are presented. The symbol size is proportional to the logarithm of the signal intensity (count rate). The sulfuric acid concentration, RH, and temperature during the nucleation period were 1.1×10^7 cm^{-3}, 37%, and 280 K, respectively. High-resolution peak fitting to CI-APi-TOF data for all nine NPF events is shown in fig. S5. Th, Thomson.

Shanghai corresponded to an almost simultaneous appearance of sulfuric acid clusters and sulfuric acid–DMA clusters. Nevertheless, the presence of sulfuric acid clusters and sulfuric acid–DMA clusters suggests that the initial growth of neutral clusters proceeded by the addition of precursor gases or preformed clusters (*6*). Apart from these clusters, a large number of organic species were observed, including highly oxygenated molecules (*31*) (table S2). Because of the extreme chemical complexity of organic species in the urban atmosphere, we were able to unambiguously assign molecular formulas to only a few of them, likely formed by reactions of peroxy radicals with NO_x or autoxidation of peroxy radicals.

The measured particle formation rates give further support for the involvement of DMA, instead of any other stabilizer, in the observed NPF events. Figure 2 shows $J_{1.7}$ against the measured [H_2SO_4] and compares these values with those measured for the H_2SO_4-H_2O, H_2SO_4-NH_3-H_2O, and H_2SO_4-DMA-H_2O nucleation mechanisms in the CERN-CLOUD experiments. Our measured particle formation rates are far higher than those derived from H_2SO_4-H_2O or H_2SO_4-NH_3-H_2O mechanisms (*10*, *27*) but close to those observed in the H_2SO_4-DMA-H_2O experiments (*9*). The average temperature (278 ± 8 K) and RH (36 ± 7%) on the NPF days during the intensive campaign are close to the CLOUD experimental conditions (278 K and 38% RH), and hence temperature and RH are not expected to substantially enhance the particle formation rates during this period in Shanghai (*32*). The average concentration of C_2-amines was measured to be 40 ± 14 pptv (parts per trillion by volume) in summer 2015 at the same sampling site (*33*), so during the intensive campaign, the DMA concentration could have reached 5 pptv, a threshold value to hit the rate limit for H_2SO_4-DMA-H_2O ternary nucleation (*9*). A similar plot for the long-term measurements with calculated [H_2SO_4] (fig. S6) also points toward the H_2SO_4-DMA-H_2O nucleation. Moreover, our NPF observation during periods with measured DMA and calculated [H_2SO_4] also indicates the important roles of H_2SO_4 and DMA in NPF (figs. S7 and S8).

Figure 3 shows that the GRs of clusters and nanoparticles during the intensive campaign increased steeply with the increasing size of clusters and particles up to 25 nm, which is consistent with the observations from long-term measurements (fig. S9). We performed cluster kinetics simulations for a collision-limited H_2SO_4-DMA system (*34*) by using the median sulfuric acid concentration and CS for the NPF events observed during the intensive campaign. The GR for sub–3-nm particles determined from simulations is on average higher than the measured GR, which means that the sulfuric acid concentrations are sufficient to explain the observed growth of sub–3-nm particles, considering that there is always a neutralizing base to stabilize sulfuric acid clusters (for instance, DMA). However, subsequent growth between 3 and 25 nm needs to be considerably boosted by organic vapors (*35*), some of which are likely detected with the CI-APi-TOF and some of which are not (fig. S10). With the typical GRs observed in Shanghai, newly formed particles reach cloud condensation nucleus sizes within a day.

On the basis of our calculations, the number of particles produced in NPF events is ~4.8 × 10^{21} km^{-2} $year^{-1}$ in the Shanghai area (see supplementary materials). This estimate is based only on the strongest NPF events, and therefore the actual value is expected to be larger. Even so, this estimate is close to the estimates of anthropogenic primary aerosol emissions (2 × 10^{22} km^{-2} $year^{-1}$) within the most polluted part of the Shanghai area (emission grid resolution of 0.5° by 0.5°) and to the average for such emissions (5 × 10^{21} km^{-2} $year^{-1}$) in the somewhat larger area (1.5° by 1.5°) (*36*) (fig. S11). Direct comparison of our results to these estimates of primary anthropogenic particle number emissions suggests that the NPF contribution to the total aerosol particle number production is about 20% in the most polluted area and 50% in a wider urban environment. However, it is notable that, according to Paasonen *et al.* (2016) (*36*), the anthropogenic particle number emissions are also highly uncertain. The authors suggest that anthropogenic emissions of nucleation-mode particles are in general underestimated because of the incomplete representation of the volatile primary particles in some observational data applied for deriving the emission factors. Because of this probable underestimation in and uncertainties related to both the NPF and the anthropogenic particle number sources, this comparison should not be taken as an estimate of the exact shares of the sources but as an indication that neither source clearly dominates over the other.

In summary, we have performed a molecular-level study of NPF events in a Chinese megacity. We detected high concentrations of sulfuric acid dimers, which point to strong acid-base

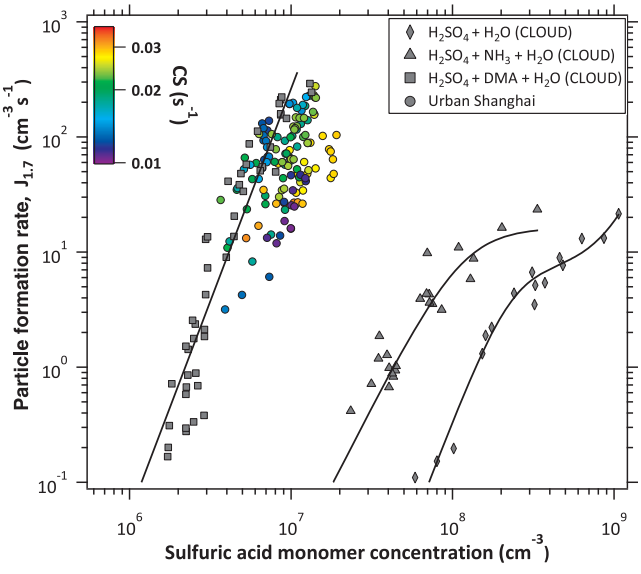

Fig. 2. Comparison of ambient and CLOUD particle formation rates against sulfuric acid monomer concentration. Gray diamonds, triangles, and squares denote CLOUD data for H_2SO_4-H_2O, H_2SO_4-NH_3-H_2O, and H_2SO_4-DMA-H_2O nucleation, respectively, at 38% RH and 278 K (*9*, *10*). The color coding denotes different CS values. The lines are plotted to guide the eye.

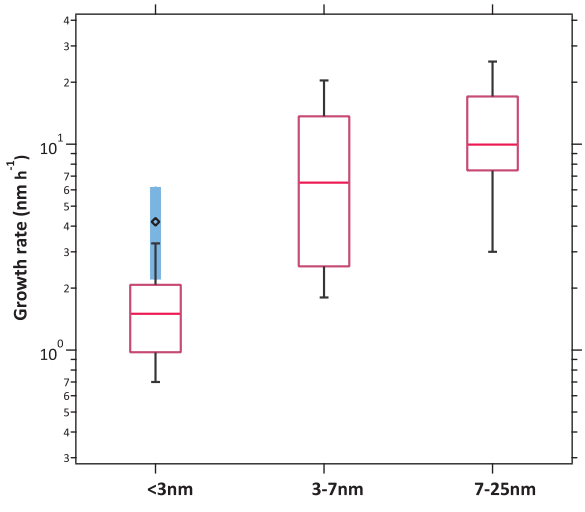

Fig. 3. Particle GRs during NPF events. GRs in different size ranges (<3 nm, 3 to 7 nm, and 7 to 25 nm) during the intensive campaign. $GR_{<3nm}$ was determined from PSM measurements, whereas $GR_{\geq 3nm}$ was calculated from nano-SMPS data. The pink horizontal lines show the median GRs, purple boxes show the 25th- and 75th-percentile values, and whiskers show the 10th- and 90th-percentile values. The black diamond shows $GR_{<3nm}$ from cluster kinetics simulations for a collision-limited H_2SO_4-DMA system with a median sulfuric acid concentration and CS for the NPF events (1.3 × 10^7 cm^{-3} and 2.1 × 10^{-2} s^{-1}). The blue box shows simulation results assuming a 50% higher or lower sulfuric acid concentration due to the uncertainty in measured H_2SO_4.

stabilization in H_2SO_4-DMA clusters. When compared to CLOUD measurements, the observed cluster formation events during our intensive campaign were consistent with H_2SO_4-DMA-H_2O nucleation, even though other mechanisms involving, for example, organic compounds could not be ruled out. Within experimental uncertainties, the sulfuric acid concentrations were high enough to result in the observed growth of sub–3-nm particles, provided that neutralizing bases, such as DMA, stabilized the sulfuric acid clusters. The exact contribution of organics and NH_3 to the growth of large clusters is yet to be elucidated. Although our results provide strong evidence for H_2SO_4-DMA-H_2O nucleation, it remains unclear how newly formed molecular clusters are able to reach sizes of a few nanometers under high CS (fig. S12), unless molecular clusters are scavenged by preexisting particles less efficiently than expected or GRs are underestimated with our current methods (*15*).

Clearly, the strong atmospheric NPF in China is a result of the vast emissions of precursor gases. NPF events in turn lead to the formation of large concentrations of new atmospheric particles that have an effect on regional air quality and potentially also the regional and global climate. For example, in the Yangtze River delta where Shanghai is located, the emissions of precursor gases, including sulfur dioxide, ammonia, and volatile organic compounds, are extremely high (*37*). In addition, the concentrations of amines (*33*, *38*) are sufficient to allow sulfuric acid particles to form at their maximum (kinetically limited) rate. Correspondingly, frequent atmospheric NPF is observed in this region (*22*, *23*). Hence, in order to reduce secondary aerosol formation in China, it is crucial to control the emissions of precursor compounds for NPF.

REFERENCES AND NOTES

1. E. M. Dunne *et al.*, *Science* **354**, 1119–1124 (2016).
2. D. V. Spracklen *et al.*, *Atmos. Chem. Phys.* **10**, 4775–4793 (2010).
3. F. Yu, G. Luo, *Atmos. Chem. Phys.* **9**, 7691–7710 (2009).
4. M. Chen *et al.*, *Proc. Natl. Acad. Sci. U.S.A.* **109**, 18713–18718 (2012).
5. Intergovernmental Panel on Climate Change, *Climate Change 2013: The Physical Science Basis* (Cambridge Univ. Press, 2013).
6. A. Kürten *et al.*, *Proc. Natl. Acad. Sci. U.S.A.* **111**, 15019–15024 (2014).
7. F. Riccobono *et al.*, *Science* **344**, 717–721 (2014).
8. S. Schobesberger *et al.*, *Proc. Natl. Acad. Sci. U.S.A.* **110**, 17223–17228 (2013).
9. J. Almeida *et al.*, *Nature* **502**, 359–363 (2013).
10. J. Kirkby *et al.*, *Nature* **476**, 429–433 (2011).
11. J. Kirkby *et al.*, *Nature* **533**, 521–526 (2016).
12. F. Bianchi *et al.*, *Science* **352**, 1109–1112 (2016).
13. M. Sipilä *et al.*, *Nature* **537**, 532–534 (2016).
14. M. Kulmala *et al.*, *Science* **339**, 943–946 (2013).
15. M. Kulmala, V. M. Kerminen, T. Petäjä, A. J. Ding, L. Wang, *Faraday Discuss.* **200**, 271–288 (2017).
16. Z. Wang *et al.*, *Sci. Total Environ.* **577**, 258–266 (2017).
17. V. M. Kerminen, M. Kulmala, *J. Aerosol Sci.* **33**, 609–622 (2002).
18. M. Kulmala, V. M. Kerminen, *Atmos. Res.* **90**, 132–150 (2008).
19. M. Kulmala *et al.*, *Boreal Environ. Res.* **21**, 319–331 (2016).
20. Z. Wu *et al.*, *J. Geophys. Res. Atmos.* **112**, D09209 (2007).
21. S. Guo *et al.*, *Proc. Natl. Acad. Sci. U.S.A.* **111**, 17373–17378 (2014).
22. S. Xiao *et al.*, *Atmos. Chem. Phys.* **15**, 1769–1781 (2015).
23. X. M. Qi *et al.*, *Atmos. Chem. Phys.* **15**, 12445–12464 (2015).
24. T. Jokinen *et al.*, *Atmos. Chem. Phys.* **12**, 4117–4125 (2012).
25. A. Hamed *et al.*, *J. Geophys. Res. Atmos.* **116**, D03202 (2011).
26. J. J. Orlando, G. S. Tyndall, *Chem. Soc. Rev.* **41**, 6294–6317 (2012).
27. A. Kürten *et al.*, *Atmos. Chem. Phys.* **16**, 12793–12813 (2016).
28. T. Petäjä *et al.*, *Phys. Rev. Lett.* **106**, 228302 (2011).
29. J. Zhao, F. L. Eisele, M. Titcombe, C. G. Kuang, P. H. McMurry, *J. Geophys. Res. Atmos.* **115**, D08205 (2010).
30. F. Bianchi *et al.*, *Environ. Sci. Technol.* **48**, 13675–13684 (2014).
31. M. Ehn *et al.*, *Nature* **506**, 476–479 (2014).
32. P. Paasonen *et al.*, *Atmos. Chem. Phys.* **12**, 9113–9133 (2012).
33. L. Yao *et al.*, *Atmos. Chem. Phys.* **16**, 14527–14543 (2016).
34. K. Lehtipalo *et al.*, *Nat. Commun.* **7**, 11594 (2016).
35. J. Tröstl *et al.*, *Nature* **533**, 527–531 (2016).
36. P. Paasonen *et al.*, *Atmos. Chem. Phys.* **16**, 6823–6840 (2016).
37. C. Huang *et al.*, *Atmos. Chem. Phys.* **11**, 4105–4120 (2011).
38. J. Zheng *et al.*, *Atmos. Environ.* **102**, 249–259 (2015).

ACKNOWLEDGMENTS

We thank the reviewers for constructive comments that improved the manuscript. We acknowledge K. Lehtipalo, L. Ahonen, and D. Stolzenburg for useful discussions. We also thank the tofTools team for providing tools for mass spectrometry analysis. **Funding:** L.W. acknowledges the National Natural Science Foundation of China (21190053, 21222703, 21561130150, and 91644213), the Ministry of Science and Technology of China (2017YFC0209505), the Cyrus Tang Foundation (CTF-FD2014001), and the Royal Society-Newton Advanced Fellowship (NA140106). M.K. acknowledges support from the Academy of Finland via his academy professorship (302958), the Academy of Finland Centre of Excellence program (projects 272041 and 307331), and the European Research Council (ERC) under the European Union's Horizon 2020 research and innovation program (ATM-GTP, grant agreement 742206). M.E. acknowledges the European Research Council (COALA, grant 638703). M.S. acknowledges the European Research Council (GASPARCON, grant 714621) and the Academy of Finland (projects 296628 and 306853). T.P. acknowledges support from the European Union's Horizon 2020 research and innovation program under grant agreement 689443 (ERAPLANET) via projects iCUPE (Integrative and Comprehensive Understanding on Polar Environments) and SMURBS (Smart Urban Solutions for Air Quality, Disasters, and City Growth) and H2020-INFRAIA-2014-2015 project ACTRIS-2 (Aerosols, Clouds, and Trace Gases Research Infrastructure) and the Academy of Finland via NanoBiomass (307537). F.B. acknowledges the Swiss National Science Foundation (grant P2EZP2_168787). O.G. acknowledges the doctoral program in atmospheric sciences (ATM-DP) at the University of Helsinki. H.J. acknowledges European Regional Development Fund project MOBTT42 under the Mobilitas Pluss program for financial support. **Author contributions:** L.W. designed the research. L.Y., F.B., J.Z., M.W., X.W., S.X., H.C., Y.L., B.Z., D.W., Q.F., F.G., L.L., H.W., L.Q., X.Y., J.C., and L.W. performed the research. L.Y., F.B., O.G., J.Z., C.Y., J.K., H.J., S.B.M., M.E., P.P., M.W., S.X., T.P., D.R.W., M.K., and L.W. analyzed the data. L.W., L.Y., O.G., F.B., and J.K. wrote the manuscript. M.E., V.-M.K., D.R.W., and M.K. edited the manuscript. All other authors commented on the manuscript. **Competing interests:** No potential conflicts of interest exist for any of the listed authors. **Data and materials availability:** All data related to this study can be obtained from the corresponding author (L.W.) via email.

SUPPLEMENTARY MATERIALS

27 July 2017; accepted 14 June 2018
10.1126/science.aao4839